Collision-energy-resolved Penning ionization electron spectroscopy of p-benzoquinone: Study of electronic structure and anisotropic interaction with He*(2 3S) metastable atoms

doi: 10.1063/1.1740740

Collision-energy-resolved Penning ionization electron spectroscopy of *p*-benzoquinone: Study of electronic structure and anisotropic interaction with He*($2\,^3S$) metastable atoms

Naoki Kishimoto, Kohji Okamura, and Koichi Ohno[a)]
Department of Chemistry, Graduate School of Science, Tohoku University, Aoba-ku, Sendai 980-8578, Japan

(Received 5 January 2004; accepted 23 March 2004)

Collision energy dependence of partial ionization cross sections (CEDPICS) of *p*-benzoquinone with He*($2\,^3S$) metastable atoms indicates that interaction potentials between *p*-benzoquinone and He*($2\,^3S$) are highly anisotropic in the studied collision energy range (100–250 meV). Attractive interactions were found around the C═O groups for in-plane and out-of-plane directions, while repulsive interactions were found around CH bonds and the benzenoid ring. Assignment of the first four ionic states of *p*-benzoquinone and an analogous methyl-substituted compound was examined with CEDPICS and anisotropic distributions of the corresponding two nonbonding oxygen orbitals (n_O^+, n_O^-) and two π_{CC} orbitals (π_{CC}^+, π_{CC}^-). An extra band that shows negative CEDPICS was observed at ca. 7.2 eV in Penning ionization electron spectrum. © *2004 American Institute of Physics.* [DOI: 10.1063/1.1740740]

I. INTRODUCTION

The electron density distribution, energy, and symmetry of specific molecular orbitals (MOs) play an important role in intermolecular processes including chemical reactions as is known in Fukui's frontier orbital theory.[1] For investigation of the energy order and symmetry of frontier orbitals, the symmetric or antisymmetric combination of atomic orbitals distributing around functional groups have been studied with a concept of through-bond/through-space intramolecular interactions.[2,3] Therefore, the assignment of ionic states and observation of the characteristics of MOs are of great importance for the study of chemical properties of molecules. However, in spite of the importance for the electronic structure of molecules, assignment of neighboring ionic states is generally difficult for many molecules by experimental studies as well as theoretical calculations.

Benzoquinones are chemically important compounds in biological systems and photochemistry because they are strong electron acceptors in charge transfer complexes. They have four important high lying occupied MOs (low ionization potentials), which are the two π_{CC} orbitals and two oxygen lone pairs (n_O).[4] 1,4-Benzoquinone (*p*-benzoquinone, PBQ) is a simple cyclic conjugated diketone and one of the most important benzoquinones. In case of PBQ the through-bond interaction between n_O orbitals, and the through-space interaction between π orbitals, and the energy of these four MOs have been extensively investigated.[4] The Hartree–Fock self-consistent-field (SCF) MO calculation of neutral PBQ gives two *g* symmetric (−) and two *u* symmetric (+) orbitals in the energy order of $\pi_{CC}^+(2b_{3u}) < \pi_{CC}^-(1b_{1g}) < n_O^-(4b_{3g}) < n_O^+(5b_{2u})$. In contrast to this, the ultraviolet photoelectron spectroscopy (UPS) of PBQ[5,6] gave IP order of $(n_O^- < n_O^+) < (\pi_{CC}^+ < \pi_{CC}^-)$. This IP order was found to be sensitive to benzenoid ring substitution.[6] It should be noted that the energy splittings between the two n_O bands and the two π bands are about 0.3 eV or smaller according to the UPS results.[6]

The assignment of observed bands of PBQ is difficult and controversial[4] mainly due to the small energy splitting mentioned above and large electron correlation effects.[7] The discrepancy between the experiment and the theory can be dissolved using experimental information of ionic states of PBQ and increasing the level of theoretical calculations.[7–11] Theoretical studies using Green's function method with two-particle-hole Tamm–Dancoff approximation (2ph-TDA),[8] CASSCF calculation,[9] and *ab initio* CI (configuration interaction) methods[7,11] with the experimental order of the four ionic states ($n_O^- < n_O^+ < \pi_{CC}^+ < \pi_{CC}^-$). Recently, observation of high resolution UPS and theoretical simulation of vibrational profile based on *ab initio* MO calculations with a vibronic coupling model performed by Stanton *et al.*[10] suggested the vertical IP order of $n_O^- < n_O^+ < \pi_{CC}^- < \pi_{CC}^+$. Their best theoretical estimation is that the two π vertical IPs are nearly degenerate around 11 eV and this qualitatively agrees with the vibrational structure. It seems that there is a general agreement in the $n_O^- < n_O^+ < (\pi_{CC}^-, \pi_{CC}^+)$ vertical IP order. The order of π_{CC} orbital is still not clearly determined. Obtaining new experimental data, which can help to assign clearly the four ionic states of PBQ (especially the two nearly degenerate states), may help understand factors affecting the ionization energy order and energy splitting. In addition to this, studying the characteristics of the four ionic states helps to get more information about the complex ionic states and the electric structure of benzoquinones.

Penning ionization ($M + He^*(2\,^3S) \rightarrow M^+ + He + e^-$) by

[a)]Electronic mail: ohnok@qpcrkk.chem.tohoku.ac.jp

collision between target M and a metastable helium atom $He^*(2\,^3S)$ provides a kinetic energy distribution of ejected electrons corresponding to each ionic state, which is known as Penning ionization electron spectra (PIES).[12–14] Although PIES are very similar to UPS, the relative band intensity of PIES are different from those in UPS.[12] In other words, branching ratios into produced ionic states differ between Penning ionization and photoionization. Photoionization cross sections obey the electric dipole selection rules,[15] whereas Penning ionization cross sections are governed by autoionization matrix elements.[16] In Penning ionization process, an electron in the respective MO to be ionized is transferred to the 1*s* orbital of He*, and the excited electron in He* is ejected, which is known as the electron exchange model proposed by Hotop and Niehaus.[17] The probability of electron transfer, therefore, largely depends on the overlap between the orbitals of M and He*, and PIES provides information on the electron distribution of individual MOs in the reactive region outside the molecular surface (boundary surface of collision between a molecule M and metastable $He^*(2\,^3S)$ atoms).[18] In this connection, quantitative estimation of PIES intensity and steric properties of MOs were studied with exterior electron density (EED) concept[18,19] outside of the molecular surface approximated by van der Waals surface. In these studies, π orbitals of aromatic compounds and lone pair orbitals were shown to be extending outside of the molecular surface and having large EED values rather than bonding σ orbitals.[18,19]

Collisional reaction dynamics in Penning ionization can be studied by detecting of products as a function of collision energy (E_c), and it enables us to investigate details of interaction potential between He* and target systems.[13] The collision energy dependence of total ionization cross sections has been measured with the detection of produced ions previously by means of velocity selection of He* beam.[20–23] In the case that the target system is an atom, where the interaction potential is isotropic, the study of the total ionization cross section is sufficient, but in the case of a molecule, where the interaction potential is anisotropic, only an averaged potential can be deduced from the collision energy dependence of total ionization cross sections. If several ionic states form in Penning ionization of a molecule, the total ionization cross section is the sum of partial ionization cross sections corresponding to each ionic state. Since a given ionic state originates from the ionization of a given MO localized on a special part of the molecule, the collision energy dependence of partial Penning ionization cross sections (CEDPICS) reflects the anisotropy of the interaction potential around the MO region.[24,25]

A combined technique of electron spectroscopy and velocity selection of He* beam with the cross-correlation time-of-flight method[26] enables us to observe a two-dimensional (collision-energy/electron-energy-resolved) Penning ionization electron spectrum (2D-PIES)[27] which includes both CEDPICS and collision-energy-resolved Penning ionization electron spectra (CERPIES).[28] For highly anisotropic systems, assignment of observed bands in 2D-PIES to MOs can be determined on the different trend of CEDPICS. For example, assignments of π bands for five-membered[29] and six-membered[30] hetero cyclic compounds and satellite bands[28–30] due to $\pi-\pi^*$ shake-up process have been discussed with the characteristic slope of CEDPICS and anisotropic interaction potential. The slope of CEDPICS for autoionization via an ion-pair potential of He^+-M^- was utilized for assignments of some extra bands observed in PIES of O_2 (Ref. 24) and CS_2 (Ref. 31) molecules.

In this study, we assigned the first four bands in PIES to pairs of *n* and π MOs on the basis of different trends of CEDPICS in 2D–PIES of PBQ and model calculations of interaction potential between PBQ and He*. In addition, since first four bands of tetramethyl-1,4-benzoquinone (TMPBQ) can be observed separately by the substitution effect,[6] different slope of CEDPICS for bands 1–4 of TMPBQ was utilized to confirm the assignment of first four bands of PBQ in PIES. Ionization process and anisotropic interactions around PBQ were also studied with the different slopes of CEDPICS.

II. EXPERIMENT

The experimental apparatus for $He^*(2\,^3S)$ PIES and He I ultraviolet photoelectron spectrum (UPS) was reported previously.[24–28,32] Metastable atoms of $He^*(2\,^1S,2\,^3S)$ were produced by a discharge nozzle source with a tantalum hollow cathode. The $He^*(2\,^1S)$ component was quenched by a water-cooled helium discharge lamp. The background pressure in a reaction chamber was on the order of 10^{-5} Pa. Sample molecules were purified under vacuum condition and admitted into a reaction chamber with gently heating. He I UPS were measured by using the He I resonance photons (584 Å, 21.22 eV) produced by a discharge in pure helium gas. The kinetic energy of ejected electrons was measured by a hemispherical electrostatic deflection type analyzer using an electron collection angle 90° to the incident $He^*(2\,^3S)$ or photon beam. The energy resolution of the electron energy analyzer was estimated to be 60 meV from the full width at half-maximum (fwhm) of the $Ar^+(^2P_{3/2})$ peak in the He I UPS. The transmission efficiency curve of the electron energy analyzer was determined by comparing our UPS data of some molecules with those by Gardner and Samson[33] and Kimura *et al.*[34] Calibration of electron energy scale was made by reference to the lowest ionic state of N_2 mixed with the sample molecule in He I UPS ($E_e=5.639$ eV)[5] and $He^*(2\,^3S)$ PIES ($E_e=4.292$ eV)[35,36] including peak energy shift of 50 meV and the difference between the metastable excitation energy and the lowest IP.

For collision-energy-resolved measurements of Penning ionization, the metastable $He^*(2\,^3S)$ beam was modulated by a pseudorandom chopper[26] rotating 400 Hz, and then introduced into a reaction cell located at 504 mm downstream from the chopper disk. Two-dimensional data $I_e(E_e,t)$ of emitted electrons from sample molecules were stored in a memory as functions of electron kinetic energy (E_e) and time (t). The resolution of the analyzer was lowered to 250 meV in order to obtain higher counting rates of Penning electrons. Another experiment for CEDPICS of overlapping bands 1–4 of PBQ was performed with higher electron energy resolution mode (ca. 60 meV). The two-dimensional spectrum can lead to the two-dimensional Penning ionization

cross section $\sigma(E_e, E_c)$ as functions of E_e and E_c (collision energy) normalized by the velocity distribution of the He*($2\,^3S$) beam. The velocity distribution of He* beam was determined by monitoring secondary electrons emitted from a stainless steel plate inserted in the reaction cell.

III. CALCULATIONS

We performed *ab initio* SCF calculations in order to obtain electron density maps. The geometries of PBQ[37] and TMPBQ[38] were selected from previous studies. For TMPBQ, D_2 symmetry was assumed. In the electron density contour maps, thick solid curves indicate the repulsive molecular surface approximated by atomic spheres of van der Waals radii.[39] In schematic diagrams of molecular orbitals, circles and ellipses were used. Solid circles indicate valence s orbitals, where couples of ellipses and dashed circles showed in-plane and out-of-plane components of *p* orbitals, respectively. Ionization potentials were calculated by outer valence Green's function (OVGF)[40] method with the partial third order calculation (P3) with the cc-pVDZ basis function in GAUSSIAN 98 program.[41]

Interaction potential $V(R)$ energy between He*($2\,^3S$) and the target molecule for various directions was also calculated on the basis of a well-known resemblance between He*($2\,^3S$) and Li($2\,^2S$); the shape of the velocity dependence of the total scattering cross section of He*($2\,^3S$) by He, Ar, and Kr is very similar to that of Li,[42] and the location of a interaction potential well and its depth are very similar for He*($2\,^3S$) and Li($2\,^2S$) with various targets.[43,44] For atomic targets (H, Li, Na, K, and Hg), quantitative estimation of the well depth was summarized to be in a good agreement with the ratio of 1.1 to 1.2 by Li model potential with respect to He*($2\,^3S$) in a recent study.[45] Due to these findings and difficulties associated with calculations for excited states, the Li atom was used in place of He*($2\,^3S$) atom. We performed interaction potential energy calculations for access of He*(Li) to PBQ and TMPBQ. By the computational limitation, 6-31+G* and 3-21+G* basis functions were adopted for PBQ and TMPBQ, respectively. The effects of electron correlations were taken into consideration by the second-order Møller–Plesset perturbation theory (MP2). Due to the strong spin contamination effect, the restricted open shell MP2 (ROMP2) method was selected for potential energy calculation for the access to the C═O group of PBQ and TMPBQ.

IV. RESULTS

Figure 1 shows the He I UPS and He*($2\,^3S$) PIES of PBQ. Figure 2 shows UPS and PIES of TMPBQ for bands 1–4. The electron energy scale for PIES is shifted relative to those for the UPS by the difference in the excitation energies, 21.22–19.82=1.40 eV. A satellite band at electron energy around 7.2 eV (IP~12.6 eV) in PIES was labeled *S*.

Figures 3 and 4 show CERPIES of PBQ and TMPBQ, respectively. In each figure, the low collision energy (average ca. 90 meV) spectra are shown by a solid curve, and the high collision energy (average ca. 250 meV) spectra are shown by a dashed curve. Figure 5 and 6 show the $\log\sigma$ versus $\log E_c$ plots of CEDPICS for PBQ and bands 1–4 of TMPBQ, respectively. The electron density maps are shown on the molecular plane, and those for π orbitals are shown on a plane at a distance of 1.7 Å (van der Waals radii of C) from the molecular plane. The CEDPICS were obtained from the two-dimensional spectrum within an appropriate range of E_e (typically the fwhm of the respective band) to avoid the effect of neighboring bands. In the Fig. 3, values of the slope parameter of CEDPICS estimated in the collision energy range of 100–250 meV by a least-squares method at each electron energy of 0.1 eV with the width of 200 meV were plotted. Shadings show band positions estimated from the slope parameter.

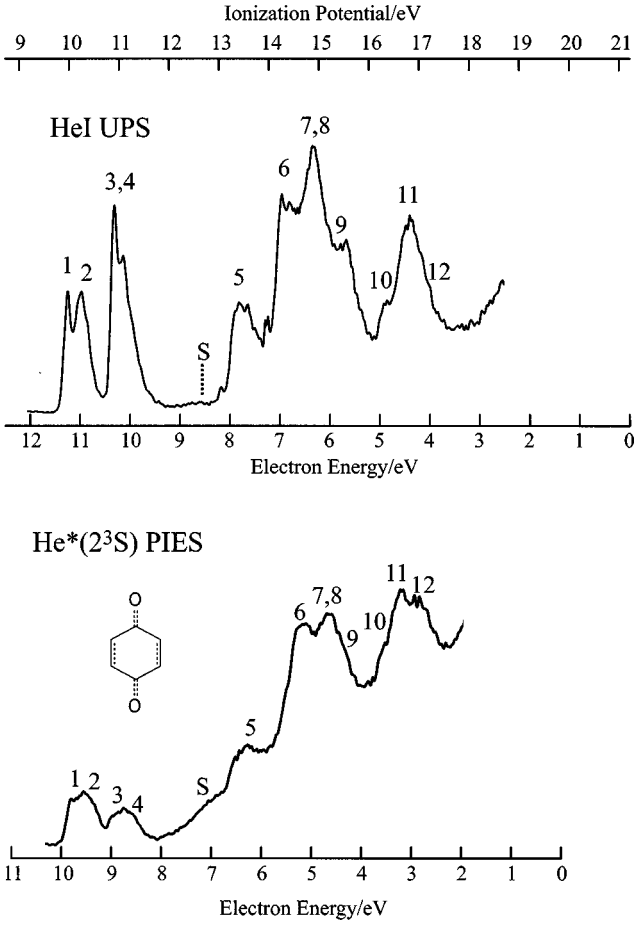

FIG. 1. He I UPS and He*($2\,^3S$) PIES of *p*-benzoquinone (PBQ).

Tables I and II list the vertical ionization potentials (IP determined from the He I UPS) and assignment of the observed bands for PBQ and TMPBQ, respectively. The orientation of PBQ in the coordinate system was fixed along with the *z* axis for C═O groups. Calculated IP values by P3, 2ph–TDA,[8] EOMIP–CCSD,[10] and SAC–CI[11] methods are listed. The peak energy shifts (ΔE) in PIES with respect to E_0 (=the difference between metastable excitation energy and target IP) are also shown. The values of peak energy shift of some diffuse bands or shoulders were shown in parentheses. Values of the slope parameter *m* for the $\log\sigma$ versus $\log E_c$ plots were estimated in the collision energy range of 100–250 meV by a least-squares method. The peak posi-

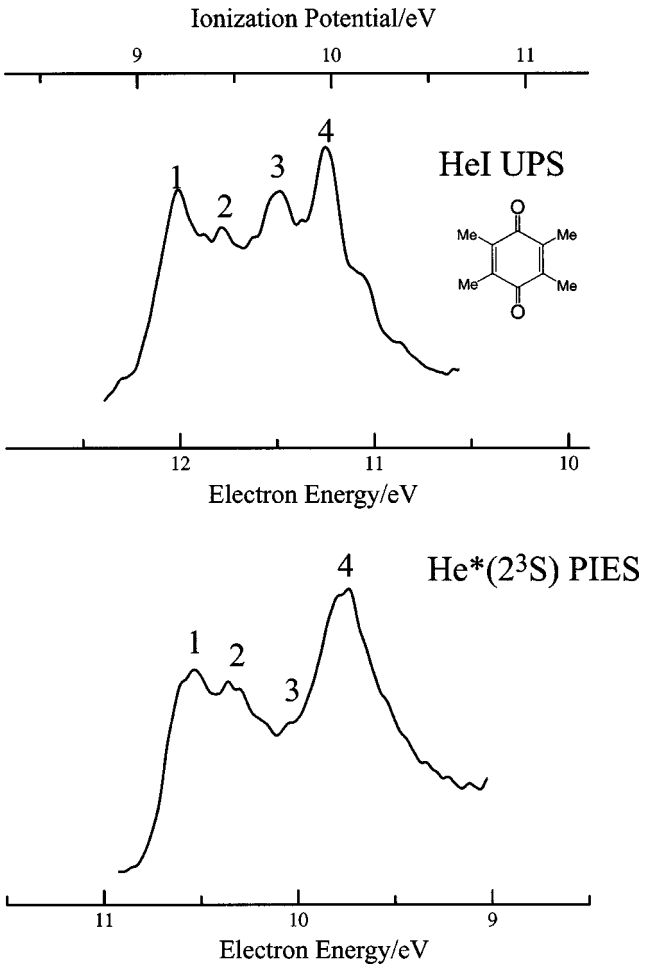

FIG. 2. He I UPS and PIES of tetramethyl-*p*-benzoquinone (TMPBQ) for bands 1–4.

tions of bands 1–4 for PBQ were determined from the change of slope *m* in Fig. 3.

Figure 7 shows model potential energy curves $V(R)$ for the access of Li atom to PBQ or TMPBQ. The distance R between the target molecule and Li is measured from the ring center $(\times)$ of the molecule. The Li–X–O angle (θ) for the

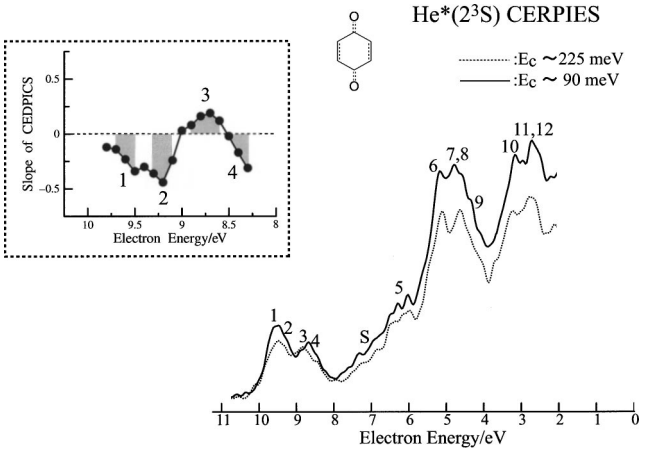

FIG. 3. Collision-energy-resolved PIES of *p*-benzoquinone (PBQ): Dashed curve at 250 meV and solid curve at 90 meV. Plot of slope parameter of CEDPICS for bands 1–4 at each electron energy with width of 200 meV is inserted. Band position estimated from the change of slope parameter was shown by shadings.

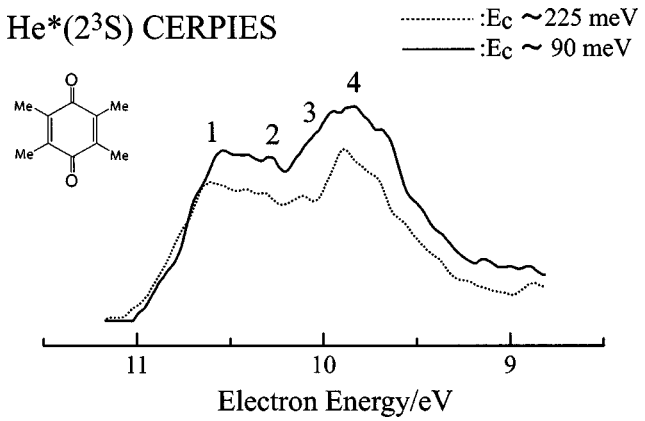

FIG. 4. Collision-energy-resolved PIES of tetramethyl-*p*-benzoquinone (TMPBQ) for bands 1–4: Dashed curve at 250 meV and solid curve at 90 meV.

out-of-plane direction was on the vertical plane to the molecular plane.

V. DISCUSSION

A. First four bands of PBQ and TMPBQ

Ionic states of PBQ[5–11,46–54] have been investigated by photoelectron spectra as well as theoretical calculations with a semiempirical (HAM/3)[54] or *ab initio* MO methods[5–11] that take the electron correlation effect into consideration. However, there are still some discussions regarding the assignment of four ionic states $(n_O^-, n_O^+, \pi_{CC}^-, \pi_{CC}^+)$ as mentioned in the introduction section (Sec. I). On the other hand, for TMPBQ, bands 1–4 in UPS were resolved by the substitution effect with four methyl groups.[6] The suggested IP order of the four bands $(n_O^- < \pi_{CC}^- < n_O^+ < \pi_{CC}^+)$[6,54] of TMPBQ was consistent with the OVGF P3 calculation in this study. For the first two ionic states of PBQ, two recent theoretical calculations (EOMIP–CCSD[10] and SAC/SAC–CI[11]) and the simulation of UPS with a vibronic coupling model[10] have indicated that the IP of the n_O^- orbital is smaller than that of the n_O^+ orbital as suggested by the UPS study utilizing substitution effects for PBQ.[6] In this study, we have also confirmed the IP order of n_O bands $(n_O^- < n_O^+)$ by observing the difference of negative slope of CEDPICS and the electron density distributions corresponding with these bands.

Since He* atoms at smaller collision energies can be attracted to the region that the MO extends (MO region) more effectively than He* atoms at higher collision energies, negative CEDPICS indicates attractive interactions[13,16,20] around the MO region. In the case of atomic targets, if the long-range attractive part of the interaction potential $V(R)$ has a function form

$$V(R) \propto R^{-s}, \tag{1}$$

the ionization cross section $\sigma(E_c)$ is represented[13,20] by

$$\sigma(E_c) \propto E_c^{-2/s}. \tag{2}$$

On the contrary, for repulsive interactions, Illenberger and Niehaus[20] showed that $\sigma(E_c)$ can be expressed as

$$\sigma(E_c) \propto [\ln(B/E_c)]^2 (E_c/B)^{(b/d)-1/2}, \tag{3}$$

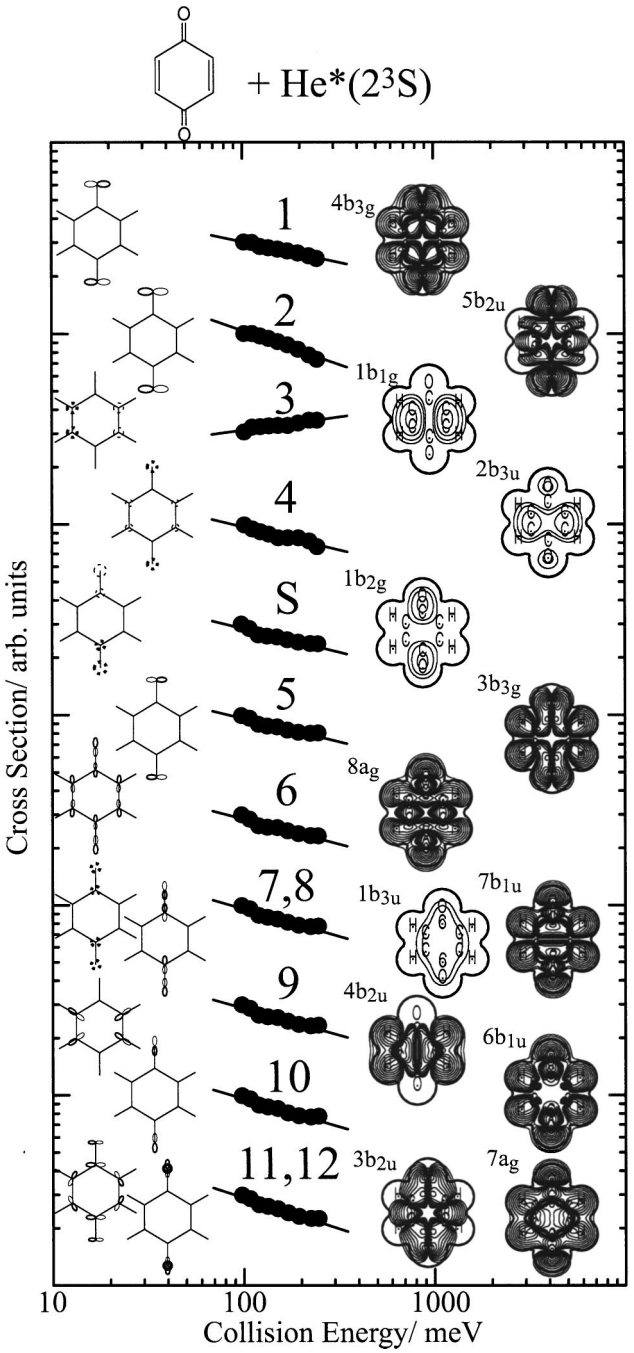

FIG. 5. Collision energy dependence of partial ionization cross sections of *p*-benzoquinone (PBQ) collided with He*($2\,^3S$).

based on the assumption of the simple forms for the interaction potential $V(R)$ and the transition probability $W(R)$ in the simple theoretical model,

$$V(R) \propto B \exp(-dR) \tag{4}$$

and

$$W(R) \propto C \exp(-bR). \tag{5}$$

The asymptotic decay of every Hartree–Fock orbital was probed to be the same except for the Be atom and the asymptotic value of the orbital exponent was shown to be equal to $(-2\epsilon_{\mathrm{HOMO}})^{1/2}$, where ϵ_{HOMO} is the orbital energy of

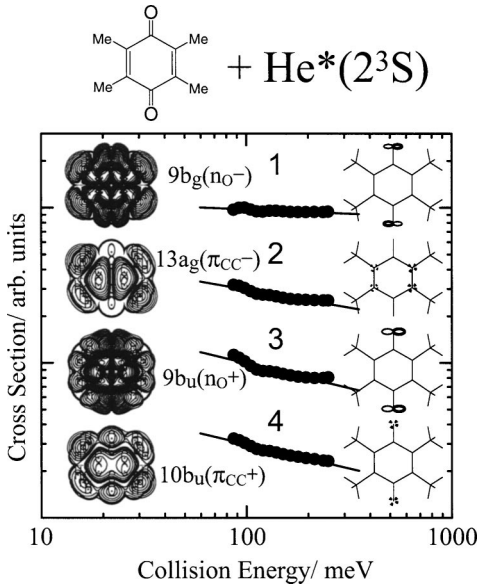

FIG. 6. Collision energy dependence of partial ionization cross sections of tetramethyl-*p*-benzoquinone (TMPBQ) collided with He*($2\,^3S$) for bands 1–4.

HOMO.[55,56] The value of b is, therefore, common for all ionic states of a given molecule M and can be expressed as

$$b = 2[2I(\mathrm{M})]^{1/2}, \tag{6}$$

where $I(\mathrm{M})$ is the lowest IP. Positive slope of CEDPICS shows that He* atoms at higher collision energies can access the inner reactive region against the repulsive wall with the effective hardness $d[=b/(m+1/2)]$.[25] If the corresponding MO extends in both repulsive and attractive interaction regions, then the slope value of the positive or negative CEDPICS shows the extent of deflection of He* atoms by repulsive and attractive interactions. The negative slope of CEDPICS for band 1 ($m=-0.21$) and band 2 ($m=-0.35$) can be ascribed to the attractive interactions around the O atoms. Further, the smaller negative slope of band 1 compared with band 2 is thought to be due to the repulsive interaction around the σ_{CH} bonds of the $4b_{3g}$ orbital region. The interaction potential calculations showed attractive wells larger than 250 meV for access of Li to the C═O group and repulsive interaction around the σ_{CH} bonds (Fig. 7). It should be noted that attractive interactions were found around the C═O group for HCHO and CH_2CHCHO (Ref. 57) or $(NH_2)_2C{=}O$ (Ref. 58) by 2D–PIES. For band 1 (n_{O}^-) and band 3 (n_{O}^+) of TMPBQ, smaller negative CEDPICS were also observed for ionization from n_{O}^- orbital ($m=-0.06$) than that for n_{O}^+ orbital ($m=-0.32$).

Peak energy shifts in PIES with respect to E_0 derived from IPs and the excitation energy of He*($2\,^3S$) can be related to the energy difference between the entrance ($\mathrm{M}+\mathrm{He}^*(2\,^3S)$) and exit channels ($\mathrm{M}^+ + \mathrm{He}$) by a two curve model.[59] When interactions for the exit channels are assumed to be very weak, large negative peak energy shifts for bands 1 and 2 of PBQ indicate that the transition occurs in the entrance channel of the attractive interaction area.

As for band 3 and band 4 of PBQ in PIES, the positive CEDPICS was observed for band 3 ($m=0.14$), while a

TABLE I. Band assignments, ionization potential (IP/eV), peak energy shift (ΔE/meV), and Slope parameter (m, see text) for *p*-benzoquinone (PBQ).

Band	IP_{Obsd}/eV	Orbital	IP_{P3}/eV (pole strength)	$IP_{2ph-TDA}$[c]/eV (pole strength)	IP_{SAC-CI}[e]/eV (intensity)	$IP_{EOMIP-CCSD}$[f]/eV	ΔE/meV	m
1	10.05	$4b_{3g}$ (n_O^-)	10.07 (0.88)	10.18 (0.82)[d]	9.57(0.898)	10.05±0.10	−170±100	−0.21[g]
2	10.23	$5b_{2u}$ (n_O^+)	10.14 (0.87)	10.71 (0.81)[d]	9.91(0.893)	10.30±0.10	−400±100	−0.35[g]
3	10.97	$1b_{1g}$ (π_{CC}^-)	11.06 (0.90)	10.89 (0.90)[d]	10.91(0.944)	11.05±0.20	−50±150	0.14[g]
4	10.97	$2b_{3u}$ (π_{CC}^+)	10.80 (0.88)	10.75 (0.85)[d]	10.66(0.931)	11.15±0.10	−450±100	−0.23[g]
S	(12.6)[a]	b	13.68 (0.82)	13.02 (0.37)	13.59(0.844)			−0.25
5	13.4	$3b_{3g}$ ($n_{O\|\|}$)	13.80 (0.87)	13.91 (0.59)	13.50(0.901)		(−130±200)	−0.24
6	14.42	$8a_g$ (σ_{CO})	14.37 (0.88)	14.49 (0.84)	14.02(0.913)		−250±150	−0.27
7,8	14.95	$1b_{3u}$ (π_{CO}^+)	14.87 (0.84)	14.80 (0.63)	14.77(0.872)		(−200±200)	−0.29
		$7b_{1u}$ (σ_{CO})	15.16 (0.88)	15.16 (0.76)	14.63(0.901)		(−200±200)	
9	15.59	$4b_{2u}$ (σ_{CH})	15.75 (0.87)	15.75 (0.85)	15.55(0.907)		(−70±200)	−0.28
10	16.45	$6b_{1u}$ (σ_{CO})	16.34 (0.86)	16.42 (0.80)	16.26(0.907)		(−130±150)	−0.30
11	16.7	$7a_g$ (σ_{CO})	16.93 (0.86)	16.99 (0.75)	16.73(0.887)		(0±200)	−0.33
12	16.9	$3b_{2u}$ (σ_{CC})	16.98 (0.85)	17.71 (0.54)	16.81(0.875)		(0±200)	

[a]Estimated from PIES.
[b]According to 2ph–TDA calculation (Ref. 8), assignment can be written as $1b_{2g}^{-1}+2b_{3u}^{-2}2b_{2g}^{1}$.
[c]Reference 8. IP values with pole strength more than 0.35 are listed.
[d]IP values by Davidson diagonalization in Ref. 8 were listed.
[e]Reference 11.
[f]Best theoretical estimate values by authors of Ref. 10.
[g]Observed in a higher electron energy resolution mode. (ca. 60 meV).

negative slope was obtained for band 4 ($m=-0.23$) as shown in the inserted plot of CEDPICS in Fig. 3 when observed in a higher electron energy resolution mode. Since the IP order of $n_O^- < n_O^+ < \pi_{CC}^+ < \pi_{CC}^-$ did not reproduce the observed vibrational structure for bands 3 and 4 in the high-resolution UPS,[10] it was finally concluded that the two π states were nearly degenerate around 11 eV of IP.[10] In the case of PIES, the larger negative peak energy shift of band 4 (−450±100 meV) compared with that of band 3 (−50±150 meV) made it possible to observe different slope of CEDPICS for band 3 and 4 in PIES. Assuming nearly degenerate π states, one can expect negative CEDPICS for band 4 rather than band 3 because of the attractive interactions in the entrance channel resulting in the negative peak shift. Although electron densities of the two π orbitals are commonly distributed either above or below carbon atoms of the benzenoid ring, the electron density of $\pi_{CC}^+(2b_{3u})$ orbital distribute not only around the carbon atoms but also around the oxygen atoms, which can be related to the attractive interaction and large negative slope for band 4 ($m=-0.23$). Model potential calculations (Fig. 7) show repulsive potential curve for the access to the center of the ring in the vertical direction, which is consistent with the positive CEDPICS of band 3 ($m=0.14$) for ionization from the $\pi_{CC}^-(1b_{1g})$ orbital. On the other hand, strong attraction of more than 1000 meV was calculated for the out-of-plane direction of PBQ for access of Li to PBQ in the angle $\theta=30°$. The deep attractive well was calculated for $R=3-4$ Å, which is located around the oxygen atom. This strong attraction is due to the short-range orbital interaction between the π_{CO}^*-type lowest unoccupied MO (LUMO) and the $2p$ orbital of Li. The negative slope of CEDPICS for the $\pi_{CC}^+(2b_{3u})$ orbital ($m=-0.23$), therefore, can be ascribed to the electron density around the oxygen atoms.

In the case of TMPBQ, the slope of CEDPICS for π_{CC}^- orbital (band 2, $m=-0.23$) is larger than that for π_{CC}^+ orbital (band 4, $m=-0.31$) as observed for PBQ in ionization from the π_{CC}^- orbital ($m=0.14$) and the π_{CC}^+ orbital ($m=-0.23$). This trend can be ascribed to the attractive interaction around the C═O groups of TMPBQ and the electron density around the C═O groups for the π_{CC}^+ MO. The attractive potential well around the C═O groups was calculated to be smaller for TMPBQ (−1.1 eV) than that for PBQ (−1.5 eV). This difference can be explained by the larger orbital energy of the π^*-type LUMO in TMPBQ (0.025 a.u. by the SCF calculation) through methyl substitution than that in PBQ (0.008 a.u.) and also by the small efficiency of the orbital interaction between LUMO of TMPBQ and the Li $2p$ orbital.

Some differences observed on comparing the PIES of TMPBQ and PBQ are as follows:

TABLE II. Band assignments, ionization potential (IP/eV), peak energy shift (ΔE/meV), and Slope parameter (m, see text) of observed bands 1–4 for tetramethyl-*p*-benzoquinone (TMPBQ).

Band	IP_{Obsd}/eV	IP_{P3}/eV (pole strength)	Orbital	ΔE/meV	m
1	9.21	9.42 (0.88)	$9b_g$ (n_O^-)	−80±100	−0.06
2	9.44	9.52 (0.90)	$13a_g$ (π_{CC}^-)	−30±150	−0.23
3	9.73	9.81 (0.86)	$9b_u$ (n_O^+)	−50±200	−0.32
4	9.97	9.88 (0.88)	$10b_u$ (π_{CC}^+)	−100±100	−0.31

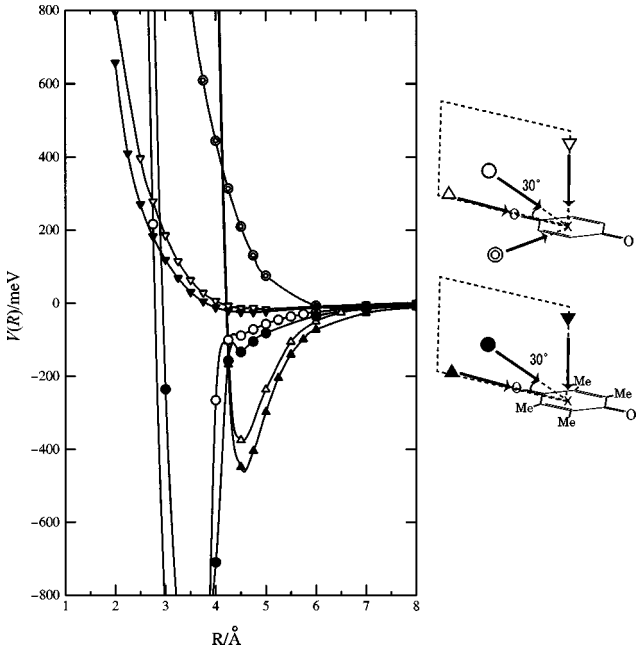

FIG. 7. Model potential energy curves $V(R)$ for the access of He*($2\,^3S$) to *p*-benzoquinone (PBQ) and tetramethyl-*p*-benzoquinone (TMPBQ) for the in-plane direction to the CH bond (◎) and out-of-plane directions vertical to the molecular plane with the angle θ of Li–X–O; $\theta=0°$ (△▲), $\theta=30°$ (○●), and $\theta=90°$ (▽▼), where R is the distance from the ring center (×) of PBQ or TMPBQ.

(1) PIES intensity of bands 3–4 (n_O^+, π_{CC}^+) is larger than that for bands 1 and 2 (n_O^-, π_{CC}^-) in TMPBQ, while the intensity of bands 1 and 2 (n_O^-, n_O^+) is larger than that of bands 3 and 4 (π_{CC}^-, π_{CC}^+) for PBQ. The in-phase extension of n_O^+ and π_{CC}^+ MOs around the molecule is favorable for Penning ionization for TMPBQ. On the other hand, attractive interactions and orbital extension around the C═O groups are effective for the ionization probability of PBQ with He*.

(2) The slopes of CEDPICS for band 1 ($n_O^-, m=-0.06$) and band 3 ($n_O^+, m=-0.32$) of TMPBQ show quite different trends, while the slopes of CEDPICS for band 1 ($n_O^-, m=-0.21$) and band 2 ($n_O^+, m=-0.35$) of PBQ show a similar negative trend. This difference also can be ascribed to the steric effect by methyl groups of TMPBQ; accessibility of He* atoms in smaller collision energies to the n_O^- orbital region of TMPBQ is thought to be reduced due to the repulsive interaction around methyl groups.

To summarize, assignment of bands 1–4 in PIES of PBQ is in the order $n_O^- < n_O^+ < \pi_{CC}^- < \pi_{CC}^+$, which is the same order that was theoretically estimated based on EOMIP–CCSD calculation and large triple excitation contribution.[10] Assuming nearly degenerate π_{CC} states as concluded by Stanton *et al.*,[10] large negative peak energy shift for ionization from the π_{CC}^+ orbital enables us to observe negative CEDPICS for band 4 in PIES due to the attractive interaction around C═O groups where the π_{CC}^+ orbital extends.

B. Assignment of bands *S* and 5

Weak band structures were reported in UPS around 13 eV in IP.[8] In this study, an extra band (*S* band) in PIES at ca. 7.2 eV in electron energy (ca. 12.6 eV in IP) showed negative CEDPICS. Since this band was not sharp, it could not have originated from H_2O. Another possible compound is hydroquinone ($C_6H_4(OH)_2$), which can be obtained from reduction of PBQ. The UPS or PIES of hydroquinone should show π bands of the benzene ring in low IP region (8.70 eV in the case of phenol[34]), though we did not observe such an extra band.

Calculated IP values for the $^2B_{2g}$ state with pole strengths in parentheses are 13.02 eV (0.37) and 14.96 eV (0.32) according to the 2ph–TDA method,[8] 13.59 eV (0.84) according to the SAC/SAC–CI theory,[11] and 13.68 eV (0.82) according to the OVGF P3 method in this study. Two theoretical calculations performed by the 2ph–TDA[8] and the SAC/SAC–CI theory[11] suggested that the $^2B_{2g}$ state corresponds to a mixed configuration of ionization from the $1b_{2g}(\pi_{CO}^-)$ MO and ionization from the $2b_{3u}(\pi_{CC}^+)$ MO with $\pi(2b_{3u})-\pi^*(2b_{2g})$ shake-up process ($1b_{2g}^{-1}+2b_{3u}^{-2}2b_{2g}^1$ by an usual expression). When we assigned the *S* band to the $^2B_{2g}$ state, the negative CEDPICS for band *S* ($m=-0.25$) may be explained by the attractive interaction around the C═O groups in ionization from the $1b_{2g}(\pi_{CO}^-)$ and $2b_{3u}(\pi_{CC}^+)$ MOs. It should be noted that the $2b_{3u}$ MO also extends around the C═O groups and shows similar negative slope of CEDPICS for band 4 ($m=-0.23$). It is known that shake-up states have a tendency to be enhanced in PIES rather than UPS and that the slope of CEDPICS for the shake-up state reflects the character of the orbital from which the electron ejected.[28,29]

Another possible ionization process for the *S* band in PIES is an electron exchange process from the $2s$ orbital of He* to π^*-type LUMO ($2b_{2g}$)[11] of PBQ and from the HOMO ($4b_{3g}, n_O^-$) of PBQ to the $1s$ orbital of He*, followed by autoionization from the HOMO of PBQ. In this case, the final ionic state is also $^2B_{2g}(4b_{3g}^{-2}2b_{2g}^1)$ state, and the electron emitted from the HOMO should lose kinetic energy being consistent with $n-\pi^*$ excitation (2.49 eV).[60] The estimated electron energy is ca. 7.28 eV ($=19.82-10.05-2.49$), which corresponds to the IP value of 12.54 eV. The slope of CEDPICS for the *S* band ($m=-0.25$) also shows a value similar to the slope of CEDPICS for n_O^- MO (band 1, $m=-0.21$).

For band 5, negative CEDPICS was obtained with a slope value of $m=-0.24$. The IP value of 13.50 eV calculated by SAC/SAC–CI theory[11] is in good agreement with the observed IP value (13.4 eV), while the IP values by using Green's function method (13.80 eV by OVGF P3 and 13.91 eV by 2ph–TDA method[8]) are relatively large for ionization from $3b_{3g}(n_{O\parallel})$ MO. Since the electron densities of $3b_{3g}(n_{O\parallel})$ MO and $4b_{3g}(n_O^-)$ MO are distributed in similar regions around the oxygen atoms, the negative CEDPICS of band 1 ($4b_{3g}, m=-0.21$) is thought to agree with that of band 5 ($m=-0.24$). The slope of CEDPICS for band 5 ($n_{O\parallel}, m=-0.24$) is less negative than that for band 2

($n_O^+, m=-0.35$) because of the repulsive interaction around the σ_{CH} bonds for the $3b_g$ ($n_{O\parallel}$) MO.

C. Bands 6–8 and 9–12 of PBQ

Negative slope values of CEDPICS from -0.2 to -0.3 were observed for bands 6–8. Ionization from σ_{CO} orbitals ($8a_g$ and $7b_{1u}$) was calculated for band 6 and band 8 by the P3 calculation, while band 7 was assigned to $\pi_{CO}^+(1b_{3u})$ orbital that extended in the out-of-plane directions. In the case of other carbonyl compounds,[57,58,61] large negative CEDPICS with a slope value of ca. -0.4 were observed for σ_{CO} bands. Nevertheless, the negative dependence of overlapping bands 6 and 7, 8 of PBQ is relatively small (-0.27 and -0.29), which can be ascribed to the repulsive interaction in the out-of-plane direction in ionization from the $\pi_{CO}^+(1b_{3u})$ orbital that extends around the center of the benzenoid ring.

Bands 9–12 were calculated to ionization from σ orbitals. The $4b_{2u}$ orbital corresponding to band 9 extends around σ_{CH} bonds where the interaction potential is repulsive. The intensity of band 9 in PIES is relatively small compared with UPS. The small ionization probability from the $4b_{2u}$ orbital is due to the repulsive interaction around σ_{CH} bonds. The negative collision energy dependence of band 9 ($m=-0.28$) in spite of the repulsive interaction can be affected by the negative CEDPICS for the overlapping bands 7, 8 ($m=-0.29$). A number of satellite lines were suggested by the 2ph–TDA method[8] in the electron energy region smaller than 4 eV. In addition, since the electron affinity of PBQ is large (about 2 eV),[62] background electrons may be observed in the electron energy region lower than 4 eV in both UPS and PIES. The qualitative trend of CEDPICS, however, can be explained by the electron distribution of MOs that contribute considerably. The negative slope of CEDPICS for band 10 ($\sigma_{CO}, m=-0.30$) can be explained by the attractive interaction around σ_{CO} bonds and the repulsive interaction around σ_{CH} bonds. Since the $3b_{2u}$ orbital scarcely extends outside the molecular surface, the negative CEDPICS of bands 11, 12 ($m=-0.33$) is mainly due to the attractive interaction around the CO group for ionization from the $7a_g$ orbital.

VI. CONCLUSIONS

Different collision energy dependence of partial Penning ionization cross sections (CEDPICS) upon collision with He*($2\,^3S$) metastable atoms was utilized to study the electronic structure of PBQ on the basis of anisotropic interaction around the molecule and the anisotropic electron density distribution of MOs to be ionized. Negative CEDPICS for n_O bands (bands 1 and 2) indicates attractive interactions around the CO groups, and relatively small negative CEDPICS of band 1 can be ascribed to repulsive interactions around the σ_{CH} bond region for ionization from n_O^- orbital.

For bands 3 and 4, although IP values for ionization from π_{CC}^- and π_{CC}^+ orbitals may be nearly the same as suggested by the theoretical simulation of vibrational structure,[10] the negative peak energy shift in PIES by the attractive interaction with He* made it possible to observe different CEDPICS for the two π_{CC} bands. The positive CEDPICS observed for band 3 can be ascribed to the repulsive interaction in vertical directions to the benzenoid ring around the π_{CC}^- orbital region. On the other hand, negative slope of CEDPICS for band 4 can be ascribed to strong attractive interaction around the CO groups in the out-of-plane directions where the π_{CC}^+ orbital has electron density. Different CEDPICS for two π_{CC} bands of TMPBQ supported the assigning of π_{CC}^- and π_{CC}^+ bands in PIES of PBQ to bands 3 and 4, respectively.

An extra band *S* was observed in PIES at 12.6 eV in IP, which was not distinctly observed in UPS. Therefore, band *S* can be ascribed to the following process: (a) mixed configuration for direct ionization from $1b_{2g}$ (π_{CO}^-) MO and π ionization accompanied by $\pi-\pi^*$ shake-up process or (b) the electron exchange from the $2s$ orbital of He* to the LUMO of PBQ and from the HOMO of PBQ to the $1s$ orbital of He*, followed by autoionization from the HOMO of PBQ. Negative CEDPICS for band *S* can be expected in both cases (a) and (b).

ACKNOWLEDGMENT

This work has been supported by a Grant-in-Aid for Scientific Research from the Ministry of Education, Culture, Sports, Science and Technology of Japan.

[1] K. Fukui, *Theory of Orientation and Stereoelection* (Springer-Verlag, Berlin, 1975).
[2] R. Hoffman, A. Imamura, and W. J. Hehre, J. Am. Chem. Soc. **90**, 1499 (1968).
[3] R. Hoffman, Acc. Chem. Res. **4**, 1 (1971).
[4] L. Klasinc and S. P. McGlynn, in *The Chemistry of Quinonoid Compounds*, edited by S. Patai and Z. Rappaport (Wiley, New York, 1988), Vol. 2, and references cited therein.
[5] D. W. Turner, C. Baker, A. D. Baker, and C. R. Brundle, *Molecular Photoelectron Spectroscopy* (Wiley, London, 1970).
[6] D. Dougherty and S. P. McGlynn, J. Am. Chem. Soc. **99**, 3234 (1977).
[7] T. Ha, Mol. Phys. **49**, 1471 (1983).
[8] W. von Niessen, L. S. Cederbaum, and J. Schrmer, J. Electron Spectrosc. Relat. Phenom. **41**, 235 (1986).
[9] M. Braga and S. Larsson, Chem. Phys. **162**, 369 (1992).
[10] J. F. Stanton, K. W. Sattelmeyer, J. Gauss, M. Allan, T. Skalicky, and T. Bally, J. Chem. Phys. **115**, 1 (2001).
[11] Y. Honda, M. Hada, M. Ehara, and H. Nakatsuji, J. Phys. Chem. A **106**, 3838 (2002).
[12] V. Čermák, J. Chem. Phys. **44**, 3781 (1966).
[13] A. Niehaus, Adv. Chem. Phys. **45**, 399 (1981).
[14] A. J. Yencha, in *Electron Spectroscopy: Theory, Technique, and Applications*, edited by C. R. Brundle and A. D. Baker (Academic, New York, 1984), Vol. 5.
[15] J. W. Rabalais, *Principles of Ultraviolet Photoelectron Spectroscopy* (Wiley, New York, 1977).
[16] W. H. Miller, J. Chem. Phys. **52**, 3563 (1970).
[17] H. Hotop and A. Niehaus, Z. Phys. **228**, 68 (1969).
[18] K. Ohno, H. Mutoh, and Y. Harada, J. Am. Chem. Soc. **105**, 4555 (1983).
[19] K. Ohno and Y. Harada, in *Theoretical Models of Chemical Bonding*, edited by Z. B. Maksić (Springer-Verlag, Berlin, 1991), Part 3.
[20] E. Illenberger and A. Niehaus, Z. Phys. B **20**, 33 (1975).
[21] M. R. Woodard, R. C. Sharp, M. Seely, and E. E. Muschlitz, Jr., J. Chem. Phys. **69**, 2978 (1978).
[22] T. P. Parr, D. M. Parr, and R. M. Martin, J. Chem. Phys. **76**, 316 (1982).
[23] L. Appolloni, B. Brunetti, J. Hermanussen, F. Vecchiocattivi, and G. G.Volpi, J. Chem. Phys. **87**, 3804 (1987).
[24] K. Mitsuke, T. Takami, and K. Ohno, J. Chem. Phys. **91**, 1618 (1989).
[25] K. Ohno, T. Takami, K. Mitsuke, and T. Ishida, J. Chem. Phys. **94**, 2675 (1991).

[26] N. Kishimoto, J. Aizawa, H. Yamakado, and K. Ohno, J. Phys. Chem. A **101**, 5038 (1997).
[27] K. Ohno, H. Yamakado, T. Ogawa, and T. Yamata, J. Chem. Phys. **105**, 7536 (1996).
[28] T. Takami and K. Ohno, J. Chem. Phys. **96**, 6523 (1992).
[29] N. Kishimoto, H. Yamakado, and K. Ohno, J. Phys. Chem. **100**, 8204 (1996).
[30] N. Kishimoto and K. Ohno, J. Phys. Chem. A **104**, 6940 (2000).
[31] S. X. Tian, N. Kishimoto, and K. Ohno, Chem. Phys. Lett. **365**, 40 (2002).
[32] T. Takami, K. Mitsuke, and K. Ohno, J. Chem. Phys. **95**, 918 (1991).
[33] J. L. Gardner and J. A. R. Samson, J. Electron Spectrosc. Relat. Phenom. **8**, 469 (1976).
[34] K. Kimura, S. Katsumata, Y. Achiba, T. Yamazaki, and S. Iwata, *Handbook of He I Photoelectron Spectra of Fundamental Organic Molecules* (Japan Scientific Press, Tokyo, 1981).
[35] D. S. C. Yee, W. B. Stewart, C. A. Mcdowell, and C. E. Brion, J. Electron Spectrosc. Relat. Phenom. **7**, 93 (1975).
[36] H. Hotop and G. Hübler, J. Electron Spectrosc. Relat. Phenom. **11**, 101 (1977).
[37] K. Hagen and K. Hedberg, J. Chem. Phys. **59**, 158 (1973).
[38] H. Schei, K. Hagen, M. Trætteberg, and R. Seip, J. Mol. Struct. **62**, 121 (1980).
[39] L. Pauling, *The Nature of the Chemical Bond* (Cornell University: Ithaca, New York, 1960).
[40] V. G. Zakrzewski and J. V. Ortiz, Int. J. Quantum Chem. **53**, 583 (1995).
[41] M. J. Frisch, G. W. Trucks, H. B. Schlegel *et al.*, GAUSSIAN 98 (Revision A.11.4), Gaussian, Inc., Pittsburgh, PA, 1998.
[42] E. W. Rothe, R. H. Neynaber, and S. M. Trujillo, J. Chem. Phys. **42**, 3310 (1965).
[43] H. Hotop, Radiat. Res. **59**, 379 (1974).
[44] H. Haberland, Y. T. Lee, and P. E. Siska, Adv. Chem. Phys. **45**, 487 (1981).
[45] H. Hotop, T. E. Roth, M.-W. Ruf, and A. J. Yencha, Theor. Chem. Acc. **100**, 36 (1998).
[46] D. O. Cowan, R. Gleiter, J. A. Hashmall, E. Heilbronner, and V. Hornung, Angew. Chem. **83**, 405 (1971).
[47] C. R. Brundle, M. B. Robin, and N. A. Kuebler, J. Am. Chem. Soc. **94**, 1466 (1972).
[48] P. E. Stevenson, J. Phys. Chem. **76**, 2424 (1972).
[49] J. E. Bloor, R. A. Paysen, and R. E. Sherrod, Chem. Phys. Lett. **60**, 476 (1979).
[50] T. Kobayashi, J. Electron Spectrosc. Relat. Phenom. **7**, 349 (1975).
[51] G. Lauer, W. Shläfer, and A. Schweig, Chem. Phys. Lett. **33**, 312 (1975).
[52] M. H. Wood, Theor. Chim. Acta **36**, 345 (1975).
[53] R. W. Bigelow, J. Chem. Phys. **68**, 5086 (1978).
[54] L. Åsbrink, G. Bieri, C. Fridh, E. Lindholm, and D. P. Chong, Chem. Phys. **43**, 189 (1979).
[55] N. C. Handy, M. T. Marron, and H. J. Silverstone, Phys. Rev. **180**, 180 (1969).
[56] M. M. Morrell, R. G. Parr, and M. Levy, J. Chem. Phys. **62**, 549 (1975).
[57] K. Ohno, K. Okamura, H. Yamakado, S. Hoshino, T. Takami, and M. Yamauchi, J. Phys. Chem. **99**, 14247 (1995).
[58] N. Kishimoto, Y. Osada, and K. Ohno, J. Phys. Chem. A **104**, 1393 (2000).
[59] A. Niehaus, Ber. Bunsenges. Phys. Chem. **77**, 632 (1973).
[60] H. P. Trommsdorff, J. Chem. Phys. **56**, 5358 (1972).
[61] N. Kishimoto, Y. Osada, and K. Ohno, J. Electron Spectrosc. Relat. Phenom. **114–116**, 183 (2001).
[62] J. Schiedt and R. Weinkauf, J. Chem. Phys. **110**, 304 (1999).